2018 European Control Conference (ECC)
June 12-15, 2018. Limassol, Cyprus

Maximizing the Electrical Efficiency of a Solid Oxide Fuel Cell System

Boštjan Dolenc[1,2], Damir Vrančič[1], Darko Vrečko[1] and Đani Juričič[1]

Abstract— **The solid oxide fuel cells (SOFCs) represent a promising technology for sustainable power generation from hydrogen rich fuels with high efficiency of energy conversion. However, only a limited number of papers address the problem of on-line maximisation of the efficiency of SOFC operation. Optimal operating conditions are normally chosen either based on experience or by using elaborated models, which are not easy to obtain. Moreover, the process changes over time due to degradation, hence the model-based performance optimisation requires on-line model update. To avoid these problems, a model-free approach is proposed. It is realised in the form of a two-tier control structure where the low-level controllers take over control of the auxiliary units around the fuel cells, while the supervisory controller (SC) controller optimises the operation point of the system. The low-level controllers are conventional feed-forward feed-back controllers, while optimisation on the higher level is solved by using the extremum seeking approach. The proposed control system is demonstrated on a simulated 10 kW SOFC system showing reliable convergence, relative rise of efficiency up to 2% and easy design and maintenance.**

I. INTRODUCTION

Solid Oxide Fuel Cells (SOFCs) hold an outstanding position in the panorama of "green" energy conversion systems owing to some fundamental advantages like high degree of fuel flexibility, high efficiency, no need for noble materials and tentative low cost of manufacturing in case of massive production [1] [2]. In the last years, more and more interest has been given to raising the reliability and efficiency of SOFC operation [3].

Unlike proton exchange membrane (PEM) fuel cells where the problem of fuel cell control has been rather well elaborated, the number of studies addressing SOFCs remains relatively limited. Some more contributions refer to the design of low-level control structures SOFCs. A feedforward-feedback control strategy for rapid load following was developed in e.g. [4], [5]. The authors noted larger (unwanted) variation of system temperatures. Similarly, Gaynor et al. [6] developed controllers that prevent fuel starvation in SOFC systems. On the other hand, Sendjaja et al. [7] describe decentralized proportional-integral (PI) control for stack voltage and fuel utilisation.

With a different objective in mind, Sorrentino et al. [8] studied the problem of proper transition between cold start and warmed-up phases. A control system for SOFC based hybrid plant, with a tubular SOFC stack and microturbine, is presented in [9]. A combination of feed-forward and feedback PI controllers is shown to keep the stack gradient as well as anode/cathode pressure difference constrained.

In what concerns optimising the performance of the SOFC system several options are explored in the literature. In these studies the SOFC systems normally make part of a wider context such as co-generation or smart grid, e.g. [10]. The authors of [11] employ feed-forward (FF)-feedback control system, similarly to [4]. The references for these controllers, however, are chosen by employing results of optimisation problem carried out off-line. Conversely, a dynamic model of the 1.5 kW SOFC power system was employed in search for optimal operating points for maximum steady state system efficiency. Jiang et al. [12] employed model-based analysis to provide the optimal open-loop for the system. The authors of [13] then used the generated data to design static FF maps to maximise system efficiency under varying load conditions. With similar control objective in mind, Li et al. [14] developed a hierarchical load tracking control of a grid-connected SOFC power system.

Considerable attention has been focused also on the design of model predictive control (MPC) controllers for e.g. load following [15]. Marchetti et al. [16] developed an MPC for real-time optimization of electrical efficiency. An experimental validation of the proposed approach is available in [17]. Within this scope, various applications of MPCs were developed employing different types of data-driven models [18], [19], [20], [21]. Although effective, the MPCs controllers rely on the accuracy of the model employed in the design. However, during operation the system dynamic properties change due to degradation processes so that a model initially derived for the new (fault-free) system becomes inaccurate, hence the control becomes ineffective.

In order to avoid laborious modelling and parameter estimation, in this paper we propose a model-free approach to the optimisation of SOFC system operation. The idea relies on a two-tier control strategy in which the low-level control loops take control over important stack variables like flows and temperatures. The overall performance optimisation concerns finding the optimum of the criterion function while respecting relevant process constraints. Instead of solving the constrained nonlinear programming problem *on the model*, we use the extremum seeking control [22] strategy on the upper level of the control hierarchy. The optimal process variables, which represent references for the low level controllers, are found by *direct optimisation on the process*. Hence even if the process changes, by direct optimisation

* The research leading to these results received funding from the European Union's Seventh Framework Programme (FP7/2007-2013) for the Fuel Cells and Hydrogen Joint Technology Initiative under grant agreement No. 621208 (Project - DIAMOND, Diagnosis-Aided Control for SOFC Power Systems). The support of the Slovenian Research Agency through Research Programme P2-0001 is gratefully acknowledged.

[1]Jožef Stefan Institute, Department of Systems and Control, Jamova cesta 39, SI-1000 Ljubljana, Slovenia, bostjan.dolenc@ijs.si

[2]Jožef Stefan International Postgraduate School, Jamova cesta 39, SI-1000 Ljubljana, Slovenia

one can keep the system operating at the optimal conditions. To the best of the authors knowledge, this is the first time that overall system operation is performed in such a model-free manner.

The ideas displayed below are evaluated by means of simulation. The simulation model of the entire process in the nominal condition is developed and implemented in Matlab.

The remainder of the paper is organised as follows. Section II provides a short description of the SOFC system, the model of which has been used to validate the proposed control approach. Section III presents the control system control system. Further on, Section IV offers validation of the control strategy based on several simulated case studies. Finally, last section contains concluding remarks.

II. SOFC SYSTEM AND ITS CORRESPONDING MODEL

The control system design and validation is carried out on a model of a SOFC system thoroughly described in [23], [24]. The system consists of balance of plant (BoP) and stack modules, as shown in Figure 1.

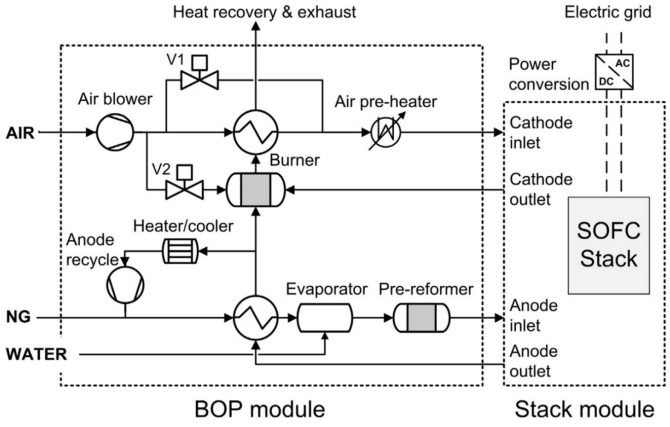

Fig. 1: System flow sheet. [24]

The stack of 80 SOFCs is enclosed in a thermally insulated casing. With 550 cm^2 of active area per cell, the stack in cross-flow configuration outputs up to 10kW of electrical power. The stack has two connecting manifolds at cathode and two at anode side. The auxiliary units (referred to as BoP), see Figure 1 consist of several interconnected components. The air blower supplies ambient air to the system. The air then passes through the heat exchanger, where it is heated up to the appropriate temperature, and then enters the cathode side. The anode air inlet temperatures can be adjusted by opening by-pass valve V1, to cool it down, or heat it up further by engaging electrical pre-heater. After leaving the stack, the cathode exhaust is then led to the catalytic afterburner, where combustion with anode exhausts is taking place. The heat produced during the combustion is recuperated via a heat exchanger. Valve V2 is a safety valve, which, if necessary, opens to prevent overheating of the afterburner.

The natural gas, fed to the anode side, is mixed with a portion of anode exhaust, drawn by anode recycle blower. This configuration, commonly known as anode off-gas recycling (AOGR), contributes significantly to the overall efficiency of power conversion, as the heat of the anode is partially recuperated. Furthermore, the exhaust is rich with water vapor required for steam reforming of the methane. Finally, the fuel gas passes through a heat exchanger and enters to the catalytic pre-reformer. In the pre-reformer, approximately 10% of the gas mixture is reformed, while the remainder is reformed directly in the stack. In the stack the electrical energy is generated through electrochemical oxidation of the hydrogen with oxygen ions which are formed in the cathode. The non-recirculated exhaust is fed to the after-burner, where it combusts with cathode exhaust.

A. The model

The first principle multiphysics model of the SOFC consists of a set of non-linear interconnected partial differential equations. These equations describe electrochemical processes, fluid dynamics and thermal processes. In this paper we adopted a lumped version of the distributed model a state-space from

$$\begin{aligned} \dot{\mathbf{x}} &= \mathbf{f}(\mathbf{x}, \mathbf{u}) \\ \mathbf{y} &= \mathbf{h}(\mathbf{x}, \mathbf{u}) \end{aligned} \tag{1}$$

where $\mathbf{x} \in R^7$, $\mathbf{u} \in R^{10}$, and $\mathbf{y} \in \mathbf{R^7}$ are state, input, and output vectors, respectively. The $\mathbf{f}(\bullet)$ and $\mathbf{h}(\bullet)$ represent sets of state-transition and output equations. The output vector consists of temperatures and molar flows at each component, and output voltage of the stack.

To keep the description brief, the model equations $\mathbf{f}(\bullet)$ and $\mathbf{h}(\bullet)$ are not described in detail in this paper. The model equations and their descriptions are available in [25], [26].

III. CONTROL OBJECTIVES AND CONTROL SYSTEM STRUCTURE

When designing the control system, the following requirements and constraints needed to be taken in to account:

1) In order to prevent hazardous electrochemical conditions that accelerate performance degradation, the SOFC system should quickly respond to changes in load. For that purpose the stoichiometric constraints, such as fuel and air utilisation, should be satisfied.
2) The stack temperatures should be kept within a prescribed interval. Too high temperatures may cause overheating and hence may harm the stack, while too low temperatures may lead to the loss of power and use of additional heating.
3) Temperature gradient over the stack should not exceed an upper bound, otherwise crack in the ceramic material as well as electrode delamination may occur.
4) The electrical efficiency of the overall system should be kept maximal.

In order to comply with the constraints and assure safe operation of the stack, the control system is split into two levels as shown in Figure 2.

The purpose of the low-level controllers is to keep the system running at corresponding operating conditions, defined

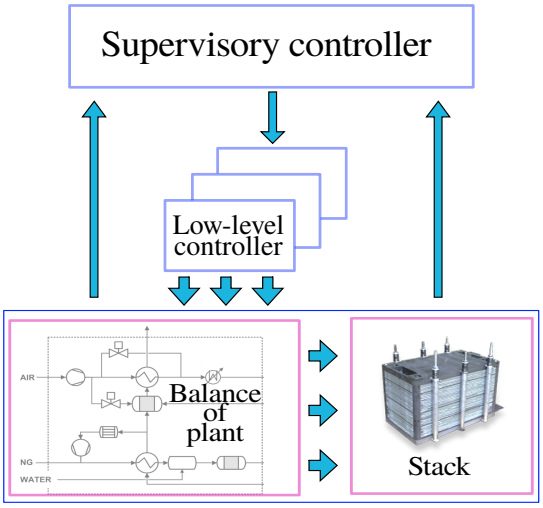

Fig. 2: The control strategy for maximisation of SOFC stack efficiency.

by the set-points. The SC calculates the system efficiency based on easily accessible process variables, as explained below, and calculates the set-points for the low-level controller in the subsequent step.

The efficiency of power conversion on the system level depends not only on the efficiency of the stack itself, but also on the power consumption of the BoP components. In order to maximise the overall electrical efficiency, one needs to minimise the power consumption of the BoP module and maximise the fuel utilisation in the stack.

Main consumers of the electrical power are air and recycle blowers, followed by the heaters and coolers. Therefore, the net system efficiency will be achieved when the air and recycle flows are minimal. The overall efficiency of the system can be effectively calculated as

$$\varepsilon = \frac{P_s - P_{ab} - P_{rb} - P_{evap} - P_{rec} - P_{ah}}{LHV\Phi_f}, \qquad (2)$$

where, referring to Figure 1, P_s is output power of the stack, P_{ab} and P_{rb} are air and recycle blower power demand respectively, and P_{evap}, P_{rec}, P_{ah} are evaporator, Heater/Cooler and air pre-heater consumptions respectively. The total energy fed to the system is calculated from flow of the natural gas Φ_f, where LHV is the lower heating value of the methane.

A. Low-level control

The purpose of this section is to briefly describe the low-level control structure shown in Figure 3. More detailed description can be found in [27], [28], while reference [20] describes the operating constraints of the system.

Note that the stack current appears as measurable disturbance, which is used in the feedforward terms in order to comply with the requirement 1. There are six main temperatures to be controlled with respect to the requirement 2. In order to find the appropriate pairing between available control inputs and controlled outputs the relative

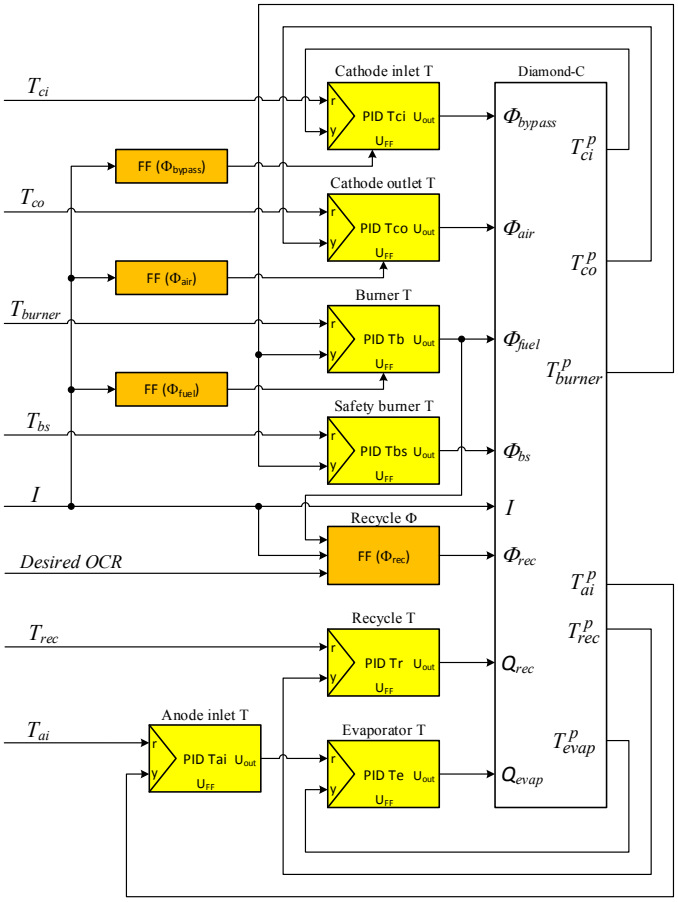

Fig. 3: The schematic representation of the low-level control system. There are six main control loops that keep the system operation in the safe region while maximising the efficiency of power conversion.

gain analysis [27] is performed. A summary of the analysis is as follows:

- *Cathode outlet air temperature* T_{co} depends on many process variables, e.g. stack current, cathode inlet air temperature and flow, anode inlet temperature and flow, the ratio of reformed fuel in pre-reformer, etc. However, out of all the manipulative variables, *cathode inlet (air) flow* $\Phi_{air,in}$ is the one with the highest relative gain, and is therefore chosen as control variable [27].
- *Cathode inlet air temperature* T_{ci} might be controlled by air pre-heater or by air by-pass valve. In order to increase efficiency and omit the use of electric pre-heater, the *air by-pass valve* Φ_{bypass} has been chosen as control variable.
- The afterburner is used to heat-up the cathode inlet flow via air heat exchanger. Its main source of energy is exhaust gas from stack, therefore the control variable is *fuel flow* Φ_f to stack, and the controlled variable is *afterburner temperature* T_{burner}. An increase of afterburner temperature is achieved by increasing the fuel flow and vice versa.

  There is another safety controller which controls after-

burner air valve V2, and prevents overheating of the catalytic burner.

- *Anode recycle flow* Φ_{rec} is controlled by FF controller that takes care about the stoichiometric conditions inside the stack. Its main purpose, given the required load, is to keep the system in theoretically carbon formation-free operating point by ensuring sufficient oxygen-to-carbon ratio (OCR) at the anode inlet.
- *Anode inlet temperature* $T_{anode,in}$ should be kept above some minimum value which usually occurs at lower stack currents. The temperature is controlled by the *evaporator temperature* T_{evap}. This is achieved by using cascade control where the inner control loop is controlling the evaporator temperature and the outer loop controls anode inlet temperature. During normal operation, the evaporator heater power is usually 0.
- *Evaporator outlet gas temperature* T_{evap} should be kept within some limits for the next stage (pre-reformer). Evaporator outlet gas temperature can be increased by the built-in *electric heater* with power Q_{evap}. In order to increase the system efficiency, the heater is usually off.
- *Anode recycle temperature* T_{rec} is controlled only to satisfy safety conditions of measuring apparatus, that is installed in the recycle loop. To facilitate proper measurements, the electrical Heater/Cooler with power Q_{rec} enables conditioning the gas passing through the pipes. The controller is activate only if the temperature exceeds corresponding upper limit.

The FF parts of the controllers, all but the recycle flow Φ_{rec}, are calculated with respect to current demand. Their main purpose is to speed-up the response of the control loop. The controllers are tuned by using the magnitude optimum approach [29]. Furthermore, all the controllers have implemented anti-windup system (due to limitations of the control variables) as well as manual/automatic control switch.

B. Supervisory control

As discussed in the previous section, the objective of the low-level controller is to keep the controlled variables at their reference values. However, the set of reference values, which is formally selected by the system operator, may be suboptimal with respect to the system efficiency. Furthermore, as the system deteriorates, the initial set at the beginning-of-life (BoL) of the system may become suboptimal. Therefore, a systematic way of adjusting the reference set is essential.

TABLE I: The set-points of the low-level controllers.

Controlled variable	Man. variable	Set-point
Ca. outlet temp. T_{co}	Air flow Φ_{air}	T_{co}
Ca. inlet temp.T_{ci}	By-pass valve Φ_{bypass}	$T_{co} \quad \Delta T(I)$
A/b out temp. T_{burner}	Fuel flow Φ_{fuel}	$T_{ci} + 120K$
Anode in temp. T_{ai}	Evap. temp. T_{evap}	720K (min)
Evap. temp. T_{evap}	Elec. heater Q_{evap}	Set by T_{ai}
OCR	Recycle flow $\Phi_{recycle}$	2.2
Anode rec. temp. T_{rec}	Electric heater/cooler Q_{rec}	800K (max)

Table I sums up the pairs of manipulated/controlled variables from Figure 3, and their corresponding set-points. It can be seen that only two variables, which define the operating point of the system, are desired OCR and cathode outlet temperature T_{co}. The remaining set points are tightly connected with the latter. For instance, the T_{ci} is set by T_{co} and current I (through FF), so that maximal temperature gradient over the stack is limited. Further, the afterburner temperature T_{burner} is defined as $T_{ci} + 120K$, so that the T_{ci} can be controlled by opening/closing the air bypass valve. To keep the system operating at high efficiency, the anode inlet controller is usually inactive, and only heats up the anode when necessary. Similarly, the T_{rec} is only controlled if needed, and is inactive during normal operation. Finally, the OCR is set to a constant value, as low as possible, so that stack operates in carbon formation free operating point while keeping the power consumption of recycle blower minimal.

The main objective of the supervisory controller is optimisation of some steady-state operating performance of the system, while at the same time satisfying some constraints. Given OCR is set fixed, it is T_{co} as the free knob to adjust efficiency. The problem of supervisory controller is the following optimisation problem

$$\begin{aligned} &\min_{T_{co}} \; c(T_{co}) \\ &T_{min} \leq T_{co} \leq T_{max} \end{aligned} \tag{3}$$

where T_{co} is approximate stack temperature, and $c(T_{co})$ is some cost function. The solution of the said problem needs to satisfy constraints, i.e. $T_{co} \in [T_{min}\ T_{max}]$.

The corresponding cost function reads

$$c(T_{co}) = (1 - \varepsilon(T_{co})) \tag{4}$$

where $\varepsilon(T_{co})$ is the efficiency at the given stack temperature T_{co}. The system efficiency $\varepsilon(T_{co})$ can be easily calculated from process variables by employing Eq. (2).

C. Extremum seeking control

To solve the optimization problem (3) the *extremum seeking* control procedure is applied. The motivation is that the conventional approaches solve the optimisation problem on system model and apply the solution to the real system. As the model of the system is inaccurate, the solution generally yields sub-optimal performance. Moreover, the system is prone to changes due to various degradation phenomena.

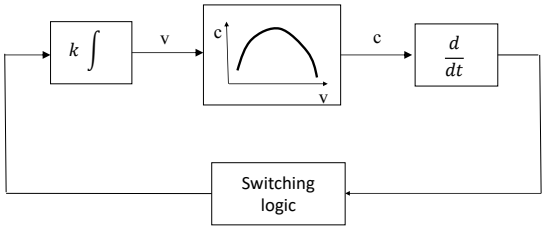

Fig. 4: A simplified view on the system from the perspective of the supervisory controller.

From the perspective of the supervisory control unit a simplified view on the entire system is shown in Fig. 4.

Assume v is argument of the criterion function $c(v)$. If we assume that the dynamics of the low level control loops is fast enough then from the supervisory point of view low level part of the system can be assumed static and hence $c(v)$ is static function. The optimum occurs at the point v^* where $\frac{\partial c}{\partial v} = 0$. If, for example, $c(v) < c(v^*)$ and the gradient $\frac{\partial c}{\partial v} > 0$ that means the value of v should be increased. The idea is to increase or decrease the argument v as a ramp with gradient $\pm k$ as long as the optimum is found.

Given that

$$\frac{\partial c}{dv} = \frac{\partial c/\partial t}{\partial v/\partial t}$$

and using results from [30] the switching logic can be expressed as follows:

$$if \ \frac{\partial c}{\partial v}\Big|_{t=t} > 0 \ then \ \frac{\partial v}{\partial t}\Big|_{t=t^+} = k \tag{5}$$

$$if \ \frac{\partial c}{\partial v}\Big|_{t=t} < 0 \ then \ \frac{\partial v}{\partial t}\Big|_{t=t^+} = -k \tag{6}$$

The unified switching rule following from the above rules reads

$$\frac{\partial v}{\partial t} = k \cdot sign \frac{\partial c}{\partial v} \tag{7}$$

One should note that the result (7) holds in case of no constraints in the argument v. In case that the limits in v are violated the rule (7) is slightly modified, i.e. if $sign \ \frac{\partial c}{\partial v}|_{t=t} > 0 \wedge v(t = t_-) = v_{max}$ then $v(t = t_+) = v_{max}$ and vice versa.

It can be easily shown that the algorithm (7) converges to the optimum. For that purpose one can analyse the Lyapunov function

$$V = \frac{1}{2}\left(\frac{\partial c}{\partial v}\right)^2 \tag{8}$$

Its time derivative reads

$$\frac{dV}{dt} = \frac{\partial c}{\partial v}\ \frac{\partial^2 c}{\partial v^2}\ \frac{\partial v}{\partial t} = \frac{\partial c}{\partial v}\ \frac{\partial^2 c}{\partial v^2}\left(k \cdot sign \frac{\partial c}{\partial v}\right) \tag{9}$$

Since $\frac{\partial^2 c}{\partial v^2} < 0$ and for any variable ξ it holds $\xi sign\ \xi > 0$ we conclude that $\frac{dc}{dt} < 0$ and hence converging to the optimum.

A discretised version of the algorithm (7) is as presented below. The pseudo-code for the applied algorithm is listed in Algorithm 1. The sampling time of the controller Δt should be long enough for the system to reach the steady-state operation. Similarly, the amplitude of the step excitation ΔT should be large enough to reflect on the efficiency. In the initial time instance, the algorithm calculates the value of the cost function $c(T_{co})$, and performs initial step change in the optimisation variable, i.e. cathode outlet T_{co} in direction d with amplitude ΔT. At the next time instance the cost function is re-evaluated and compared to its value from the previous time instance. If its value is decreased, than the algorithm continues with step changes in the same direction. Alternatively, the direction of search is reversed, and reference is changed with amplitude of two steps.

IV. Evaluation of the proposed control system

The evaluation of the proposed control system is carried out in simulated process model in Matlab environment.

while $t = k\Delta t$ **do**
  if *step* **then**
    $T_{co}(k) = T_{co}(k-1) + d\Delta T$
    $step = 0$
  else if $c(k\Delta t) < c((k-1)\Delta t)$ **then**
    $T_{co}(k) = T_{co}(k-1) + d\Delta T$
    $step = 1$
  else
    $d = -d$;
    $T_{co}(k) = T_{co}(k-1) + 2d\Delta T$
    $step = 1$
  end
end

Algorithm 1: P&O algorithm.

A. Analysis of the cost function on system level with implemented low-level controller

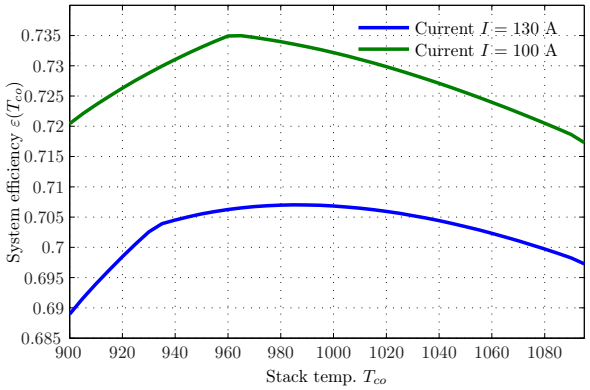

Fig. 5: Analysis of performance criteria on the system level with implemented low-level controller.

Figure 5 shows the efficiency of the system as a function of stack temperature T_{co}. The load current was kept constant at two points, $I \in \{100, 130\}$ A, while the stack reference T_{co} was increasing in linear manner from minimal to maximal allowed values. Note that enough time was left between two consecutive increases in T_{co} so that the transients behavior of the system was over and only steady-state values were obtained. Two facts are apparent from the Figure 5:

(i.) efficiency of power conversion with increasing reference temperature of the stack first increases and then decreases.;

(ii.) system efficiency is heavily dependent on the stack current.

The explanation of such a behavior of the system is as follows. In order to achieve lower, or higher temperatures of the stack, two opposing actions are applicable: (i.) less air is fed to the system to cool it down, air blower consumption is reduced, and efficiency increases; (ii.) if heat production due to hydrogen oxidation is insufficient, more fuel is required to heat up the system, and efficiency drops. The analysis shows

that the system efficiency can be improved by 2% by only selecting proper operating point. Moreover, the efficiency as a function of temperature seems to "flatten" a with increasing loads and, on average, decreases.

B. Results and discussion

A simulation study was performed to illustrate the benefits of the supervisory controller (SC). During the simulation the current was kept at 100 A up until ca. $t = 120$ h. At that point, the current was ramped up to 130 A. Figure 6 shows the actions of the SC, and corresponding response of the system, i.e. the system efficiency. The operating constraints for the system were $T_{min} = 900K$ and $T_{min} = 1100K$. The initial starting point for the system was selected at lower boundary $T = 900K$, as it is preferred to keep the system at lower temperatures. The sampling time of the SC Δt was selected so that transient of the system was over between two consecutive actions i.e. $\Delta t = 4$h. The incremental step change in stack temperature was selected first $\Delta T = 5$ K. From the beginning the SC started increased

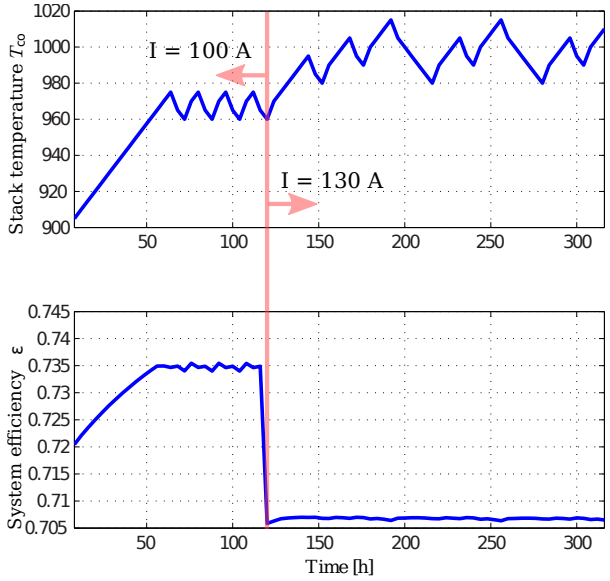

Fig. 6: Simulated results for $\Delta T = 5$ K: the SC increased the temperature to reach the optimal operating point.

the stack temperature up to 960 K. This point corresponds well to the maximum in Figure 5 – see green curve that corresponds to 100 A load. From that point on, the SC kept stack temperature fluctuating around optimum. At ca. $t = 120$ h, the load was increased to 130 A. Again, the stack temperature was incrementally increased up in order to maximise the efficiency. Note that at different stack current the dependency of system efficiency on temperature changes significantly. At load $I = 130$ A, the concavity of the criterion function is not as pronounced as it is at $I = 100$ A. This, in combination with large optimisation step $\Delta T = 5$ K causes large oscillation in the stack temperature, as shown in the figure from $t = 120$ h on.

In order to decrease such a large variation is stack temperature, one can select smaller optimisation step, e.g. $\Delta T = 1$ K. The same simulation, only with smaller step size, can be seen in Figure 7. The results again show that the optimum is reached, even after the transient. However, the optimisation took significantly more time to converge.

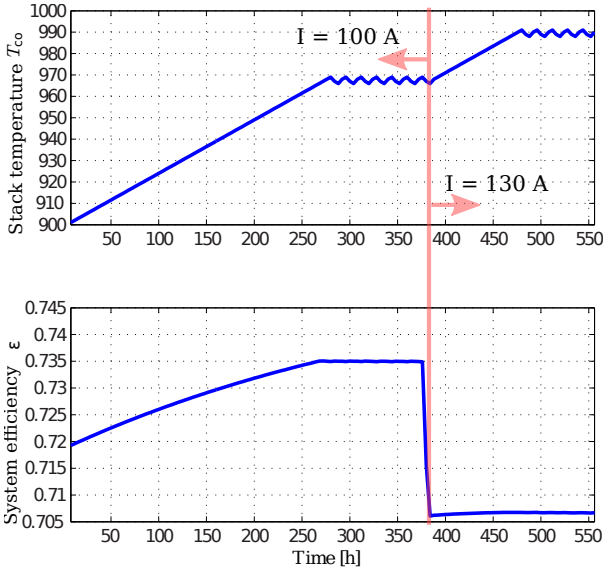

Fig. 7: Simulated results for $\Delta T = 1$ K: the SC increased the temperature to reach the optimal operating point. The oscillations are significantly decreased with smaller ΔT at the cost of slower convergence.

V. Conclusion

The paper presents a control system to optimally operate SOFCs systems. The control architecture is split into two layers i.e. low-level controllers and and supervisory controller. The low-level controllers are designed to minimise the electric consumption of the BoP components while at the same time keeping the stack operating in safe regime. The supervisory controller adjusts the optimum stack temperature to maximise efficiency by means of extremum seeking. It is shown that the supervisory controller converges to the optimum. The improvement in efficiency in that case can be cca. 2%.It is important to stress that the entire controller is designed without using the process model.

The proposed control system is validated on a model of a 10 kW SOFC system. The results show that overall efficiency of the system can be risen by 2% solely by selecting appropriate operating point of the system. It is shown that the optimisation converges to true solution, and that the convergence rate heavily depends on the parameters of the optimisation algorithm.

References

[1] A. B. Stambouli and E. Traversa, "Fuel cells, an alternative to standard sources of energy," *Renew. Sustainable Energy Rev.*, vol. 6, pp. 297–306, 2002.

[2] A. Kirubakaran, S. Jain, and R. Nema, "A review on fuel cell technologies and power electronic interface," *Renew. Sustainable Energy Rev.*, vol. 13, pp. 2430–2440, 2009.

[3] M. Atanasiu, "The status of sofc r&d in the fuel cell and hydrogen joint undertaking program," *ECS Trans.*, vol. 68, pp. 3–14, 2016.

[4] F. Mueller, F. Jabbari, R. Gaynor, and J. Brouwer, "Novel solid oxide fuel cell system controller for rapid load following," *Journal of Power Sources*, vol. 172, no. 1, pp. 308 – 323, 2007.

[5] M. Carré, R. Brandenburger, W. Friede, F. Lapicque, U. Limbeck, and P. da Silva, "Feed-forward control of a solid oxide fuel cell system with anode offgas recycle," *J. Power Sources*, vol. 282, pp. 498 – 510, 2015.

[6] R. Gaynor, F. Mueller, F. Jabbari, and J. Brouwer, "On control concepts to prevent fuel starvation in solid oxide fuel cells," *J. Power Sources*, vol. 180, no. 1, pp. 330 – 342, 2008.

[7] A. Y. Sendjaja and V. Kariwala, "Decentralized control of solid oxide fuel cells," *IEEE Transactions on Industrial Informatics*, vol. 7, no. 2, pp. 163–170, May 2011.

[8] M. Sorrentino and C. Pianese, "Model-based development of low-level control strategies for transient operation of solid oxide fuel cell systems," *Fuel Cells Science & Technology 2010*, vol. 196, pp. 9036–9045, 2010.

[9] M. Ferrari, "Advanced control approach for hybrid systems based on solid oxide fuel cells," *Appl. Energy*, vol. 145, pp. 364 – 373, 2015.

[10] A. Hajizadeh and M. A. Golkar, "Intelligent power management strategy of hybrid distributed generation system," *Int. J. Elec. Pow.*, vol. 29, no. 10, pp. 783 – 795, 2007.

[11] H. Cheng, S. Jing, Y. Xu, Z. Deng, J. Li, and X. Li, "Control-oriented modeling analysis and optimization of planar solid oxide fuel cell system," *Int. J. Hydrogen Energy*, vol. 41, no. 47, pp. 22 285 – 22 304, 2016.

[12] J. Jiang, X. Li, and J. Li, "Modeling and model-based analysis of a solid oxide fuel cell thermal-electrical management system with an air bypass valve," *Electrochim. Acta*, vol. 177, pp. 250 – 263, 2015.

[13] L. Zhang, J. Jiang, H. Cheng, Z. Deng, and X. Li, "Control strategy for power management, efficiency-optimization and operating-safety of a 5-kW solid oxide fuel cell system," *Electrochim. Acta*, vol. 177, pp. 237 – 249, 2015.

[14] Y. Li, Q. Wu, and H. Zhu, "Hierarchical Load Tracking Control of a Grid-Connected Solid Oxide Fuel Cell for Maximum Electrical Efficiency Operation," *Energies*, vol. 8, no. 3, pp. 1–21, March 2015.

[15] L. T. Jacobsen, B. J. Spivey, and J. D. Hedengren, "Model predictive control with a rigorous model of a solid oxide fuel cell," in *2013 American Control Conference*, June 2013, pp. 3741–3746.

[16] A. Marchetti, A. Gopalakrishnan, B. Chachuat, D. Bonvin, L. Tsikonis, A. Nakajo, Z. Wuillemin, and J. Van Herle, "Robust real-time optimization of a solid oxide fuel cell stack," *J. Fuel Cell Sci. Technol.*, vol. 8, no. 5, 2011.

[17] G. Bunin, Z. Wuillemin, G. Francois, A. Nakajo, L. Tsikonis, and D. Bonvin, "Experimental real-time optimization of a solid oxide fuel cell stack via constraint adaptation," *Energy*, vol. 39, no. 1, pp. 54 – 62, 2012.

[18] X. Wang, B. Huang, and T. Chen, "Data-driven predictive control for solid oxide fuel cells," *J. Process Control*, vol. 17, no. 2, pp. 103 – 114, 2007.

[19] H.-B. Huo, X.-J. Zhu, W.-Q. Hu, H.-Y. Tu, J. Li, and J. Yang, "Nonlinear model predictive control of SOFC based on a Hammerstein model," *J. Power Sources*, vol. 185, no. 1, pp. 338 – 344, 2008.

[20] A. Pohjoranta, M. Halinen, J. Pennanen, and J. Kiviaho, "Model predictive control of the solid oxide fuel cell stack temperatur with models based on experimental data," *J. Power Sources*, vol. 277, pp. 239–250, 2015.

[21] X.-J. Wu, X.-J. Zhu, G.-Y. Cao, and H.-Y. Tu, "Predictive control of SOFC based on a GA-RBF neural network model," *J. Power Sources*, vol. 179, no. 1, pp. 232 – 239, 2008.

[22] K. Ariyur and M. Krstic, *Real-Time Optimization by Extremum-Seeking Control*. Wiley, 2003.

[23] A. Pohjoranta, M. Halinen, J. Pennanen, and J. Kiviaho, "Solid oxide fuel cell stack temperature estimation with data-based modeling - designed experiments and parameter identification," *J. Power Sources*, vol. 277, p. 464–473, 2015.

[24] M. Halinen, M. Rautanen, J. Saarinen, J. Pennanen, A. Pohjoranta, J. Kiviaho, M. Pastula, B. Nuttall, C. Rankin, and B. Borglum., "Status of SOFC demonstration unit with 10 kW stack," *ECS Trans.*, vol. 35, pp. 113–120, 2011.

[25] B. Dolenc, P. Boškoski, M. Stepančič, A. Pohjoranta, and Juričić, "State of health estimation and remaining useful life prediction of solid oxide fuel cell stack," *Energy Convers. Manag.*, vol. 148, pp. 993 – 1002, 2017.

[26] D. Marra, C. Pianese, P. Polverino, and M. Sorrentino, *Models for Solid Oxide Fuel Cell Systems: Exploitation of Models Hierarchy for Industrial Design of Control and Diagnosis Strategies*. Springer, 2016.

[27] D. Vrečko, G. Dolanc, B. Dolenc, D. Vrančić, B. Pregelj, D. Marra, M. Sorrentino, C. Pianese, A. Pohjoranta, and Juričić, "Feedforward-feedback control of a SOFC power system: A simulation study," *ECS Trans.*, vol. 68, pp. 3151–3163, 2015.

[28] D. Vrečko, M. Nerat, D. Vrančić, G. Dolanc, B. Dolenc, B. Pregelj, F. Meyer, S. Au, R. Makkus, and Juričić, "Feedforward-feedback control of a solid oxide fuel cell power system," *Int. J. Hydrog. Energy*, 2018 - To appera.

[29] D. Vrancic, D. Vrecko, B. Dolenc, and Juričić, "Design of low-level controllers for diamond-c system. diamond project deliverable 5.1," Tech. Rep., 2016.

[30] H.-T. Yau and C.-H. Wu, "Comparison of extremum-seeking control techniques for maximum power point tracking in photovoltaic systems," *Energies*, vol. 4, pp. 2180–2195, 2011.